Dynamic Simulation of Central Chilling System of A Large Office Building

Shengwei Wang, Jinbo Wang, John Burnett

Department of Building Services Engineering
The Hong Kong Polytechnic University, Kowloon, Hong Kong

Abstract

Dynamic simulation of a seawater-cooled chilling system is performed by using the dynamic models of centrifugal chillers, heat exchangers, seawater and chilled water networks, cooling coil, actuator, sensor, variable-speed pump and DDC controller of BEMS. The on-line control strategies for the central chilling system are tested and evaluated by using them to control the living chilling system under different AHU dynamic loads in four seasons. This paper presents the models developed to simulate the dynamic system, the on-line control strategies developed for the chilling system and the evaluation of the strategies by system dynamic simulation.

Introduction

Buildings are the largest energy consumers in Hong Kong. The limited fresh water resources and Government restrictions on use for cooling towers have resulted in Hong Kong having the most seawater cooling systems world wide. Variable-speed seawater pumps have been used in many seawater cooled chilling systems. Improving energy efficiency of centralized chilling systems will significantly reduce the total energy consumption in large office buildings. The HVAC (Heating, Ventilating and Air-Conditioning) system simulation is not only a useful tool to evaluate/improve the building air-conditioning system design but also an efficient tool in improving the energy efficiency of the HVAC system by optimizing or improving the system operation and control [1,2].

In order to test and upgrade the on-line control strategies of seawater-cooled central chilling systems, dynamic models of centrifugal chillers, heat exchangers, seawater and chilled water networks, cooling coil, actuator, sensor, variable-speed pump and frequency inverter, DDC (Direct Digital Control) controller of BEMS (Building Energy Management System) are developed to simulate the realistic (e.g. thermodynamic, hydraulic, energy and control) performances of the chilling system controlled by on-line control strategies. To represent the dynamic cooling load of chilling system from the Air Handling Units (AHU) in the building, the AHUs controlled by DDC are included in simulation.

Simulation exercise was performed on the dynamic system simulated to test and evaluated the on-line control performance of BEMS local and supervisory strategies in different seasons. The energy and control performances of derivative and adaptive control strategy for the on-line optimal seawater pressure set-point reset was tested and evaluated.

This paper presents the models developed to simulate the dynamic system including the thermodynamic and hydraulic performances of seawater network chilling plants and

secondary chilled water network. It also presents the control strategies developed for the chilling system and the evaluation of the on-line strategies by dynamic system simulation.

System Description

The studies presented in this paper are performed on the chilling system in a large office building in Hong Kong. The building has 46 stories and a usable area of about 74000 m^2 . The central chilling system is located at the basement with the seawater pump station at the sea front about 500 meters away.

The central plant (Figure-1) consists of five identical indirect seawater-cooled centrifugal chillers using R-12, three variable speed seawater pumps, and two auxiliary heat exchangers. Four of the chillers serve for normal duty and one for stand-by. The design cooling capacity of each chiller is 3100 kW. Two of the pumps are duty pumps and one is for stand-by. One auxiliary heat exchanger is used (the second is for stand-by) twenty-four hours a day serving the essential A/C units in a number of important rooms, such as computer centers. Each chiller is associated with one constant condenser water pump and one constant primary chilled water pump. There are four constant secondary chilled water pumps (three for duty and one for stand-by). The seawater pump speed is controlled by moderating the frequency input using one frequency inverter for each of the pump.

A few office floors are in use twenty-four hours a day including public holidays. Therefore, the chilling system operates continuously and the load on the chillers varies significantly even within one day. The pressure control of the seawater system, the AHU supply air temperature control and the BEMS monitoring points essential for the BEMS control strategies are shown in the figure.

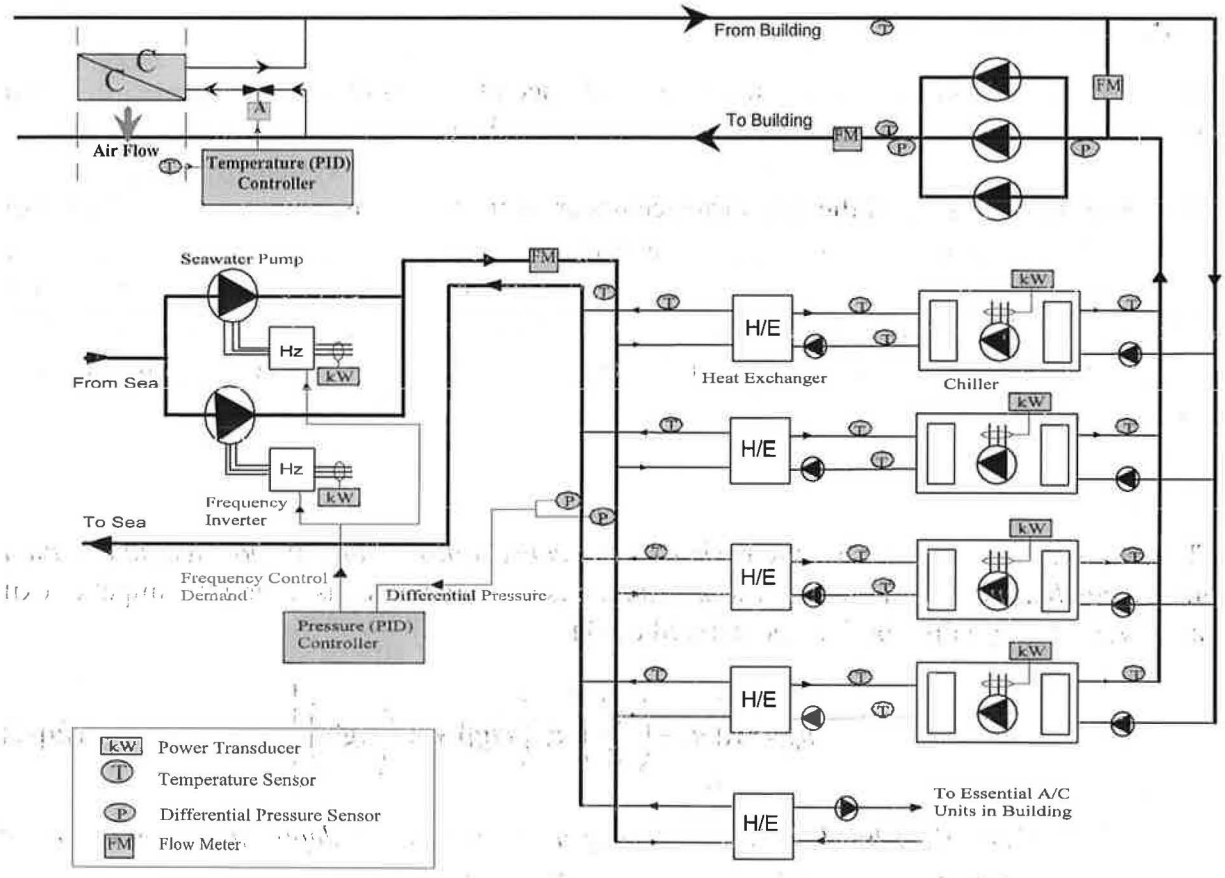

Figure-1 Central chilling system and chilled water network
with measurement points essential for BEMS control

The cooling of the offices is served by the Air Handling Units at each office floor (only the control loop of one AHU cooling coil is shown in Figure-1). The supply air temperature after a cooling coil is control by a PID temperature controller in a typical AHU, which adjusts the chilled water flow rate through cooling coil by moderating the two way moderating valve.

The differential seawater pressure between supply and return pipes near heat exchangers is monitored and controlled by a DDC controller. The PID pressure controller controls the pressure by moderating the frequency of the AC power input to the pumps. The AC power input frequency to the two pumps are set to be the same to share the load equally.

The instantaneous power consumption of each chiller and seawater pump is measured by a kW transducer. The differential pressure of the supply water and return water pipes near the exchangers is measured by differential pressure sensors. The supply seawater temperature at the supply pipe is also measured. The return seawater temperature after each exchanger, the condenser cooling water temperatures at the inlet and outlet of each exchanger are measured to monitor the performance of the heat exchangers. The chilled water temperature, the chilled water temperatures to/from building, the chilled water flow rate to building, the water flow rate through bypass pipe, the differential pressure across the secondary pumps, and the seawater flow rate are monitored by BEMS.

Chilling System Component Models

Centrifugal Chiller

The chiller model simulates the dynamic performance of single- or multi-stage water- cooled centrifugal chillers using a steady-state approach [3] and a dynamic approach.

The model simulates the chiller performance under various working conditions on the base of impeller tip speed (u_2), impeller exhaust area (A), impeller blades angle (β) and thirteen other coefficients/constants, which might be available from chiller technical data or identified (partially or fully) by an associated preprocessor using chiller performance data under full load and partial load. The chiller capacity is assumed to be controlled by adjusting the inlet vane angle (θ).

Compressor

The compressor is modeled on the basis of *mass conservation, Euler turbomachine equation* and *energy balance equation*. The Euler equation is modified by considering the impeller exit radial velocity (c_{r2}) distribution and derived as (1).

$$h_{th} = u_2\left[u_2 - \left(\frac{\pi^2}{8}\right)^2 c_{r2}\left(ctg\beta + B\frac{v_1}{v_i}tg\theta\right)\right] \quad \text{(Eq-1)}$$

where, h_{th} is theoretical head, B is the ratio of impeller channel depth at intake to that at exhaust, v_1 and v_i are specific volume at impeller intake and exhaust respectively.

Energy balance equations (polytropic compression work (h_{pol}), hydrodynamic losses (h_{hyd}), etc.) are applied to two control volumes, i.e. compressor control volume (from compressor suction to compressor exhaust) and impeller control volume impeller (from compressor suction to impeller exit) as shown in (2) and (3).

$$h_{th} = h_{pol.comp} + h_{hyd.comp} \quad \text{(Eq-2)}$$

$$h_{th} = h_{pol.imp} + h_{hyd.imp} + \frac{c_i^2}{2} \quad \text{(Eq-3)}$$

where, c_i is the vapor velocity at impeller exhaust.

Hydrodynamic Losses (h_{hyd}) in two control volumes are considered to be composed of three elements, i.e. flow friction losses, inlet losses and incidence losses as shown in (4) and (5). The flow friction losses is considered proportional to the compressor volume flow rate squared and thus proportional to the impeller exit radial velocity squared (c^2_{r2}). The inlet losses are considered proportional to the velocity through prerotation vanes channel squared (c^2_{van}). Incidence losses is considered proportional to the shock velocity component squared (c^2_{ul}).

$$h_{hyd.comp} = \varsigma\left[1 + \psi_1\left(\frac{v_1}{v_i}\frac{1}{\cos\theta}\right)^2 + \psi_2\left(\frac{v_1}{v_i}\mathrm{tg}\theta\right)^2\right]c_{r2}^2 \quad \text{(Eq-4)}$$

$$h_{hyd.imp} = \varsigma\left[\chi + \psi_1\left(\frac{v_1}{v_i}\frac{1}{\cos\theta}\right)^2 + \psi_2\left(\frac{v_1}{v_i}\mathrm{tg}\theta\right)^2\right]c_{r2}^2 \quad \text{(Eq-5)}$$

where, ζ,, ψ_1, ψ_2, χ are the introduced constants.

Given the evaporator pressure, condenser pressure and position of inlet vanes (value of θ), the compressor model can calculate radial velocity and specific volume at impeller exhaust, thus, refrigerant mass flow rate and internal power. The compressor capacity is controlled by the inlet vanes angle (θ) as shown in equation (4) and (5).

In multi-satge chiller model, single stage compressor equations are used to calculate the first stage. The second stage is assumed to have the same flow efficiency and compression ratio as the first stage. Mass and energy conservations are applied to the economizer and the mixing process at the second stage suction. Only the first stage impeller geometric parameters are of concern.

Condenser and evaporator

Evaporator and condenser are simulated using the classical heat exchanger efficiency method. By considering the effects of water flow rate ($W_{w,ev}$, $M_{w,cd}$) and heat flux (Q_{ev}, Q_{cd}), the evaporator and condenser overall heat transfer coefficients (UA_{ev}, UA_{cd}) are represented empirically as shown by (6) and (7), which represent the effects of the water flow rate on the heat convection on water side and the effects of heat flux on the boiling and condensation processes on the refrigerant side [4].

$$UA_{ev} = \left[C_1 M_{w,ev}^{-0.8} + C_2 Q_{ev}^{-0.745} + C_3\right]^{-1} \quad \text{(Eq-6)}$$

$$UA_{cd} = \left[C_4 M_{w,cd}^{-0.8} + C_5 Q_{cd}^{1/3} + C_6 \right]^{-1} \qquad \text{(Eq-7)}$$

where, C_1 - C_6 are constants.

The evaporation and condensation temperatures, and thus the evaporator and condenser pressures are calculated, given chilling capacity (Q_{ev}), heat rejection (Q_{cd}), chilled and cooling water flow rates and inlet temperatures,.

Power consumption

Chiller power consumption (W) is calculated on the basis of the compressor internal power (W_{in}). With the consideration of compressor mechanical and leakage losses, motor electrical and mechanical losses, the chiller power consumption is the sum of three components, i.e., the internal compression power (W_{in}), a variable part of the losses which is proportional to the internal compression power, and a constant part of the losses W_l. as shown in (7).

$$W = \alpha \cdot W_{in} + W_l \qquad \textit{(Eq-8)}$$

where, α is a coefficient which is a constant for a chiller.

Model parameters identification

Of the model parameters, impeller geometric parameters (U_2, A, β) are either given by manufacturer or, together with the other parameters, identified according to the performance data given by manufactures or from field measurements. Parameter identification is carried out by a preprocessor associated with the model.

Dynamics model of chiller

The dynamics of the chiller is simulated by assuming two thermal storages, one at the cooling water inlet of condenser and the another at the chilled water inlet of evaporator as shown in Figure-2 and mathematically represented by two first order differential equations (9) and (10). This simple approach reasonably presents both the dynamic response of chiller to the change of working conditions (inlet temperatures) and the dynamic effects of the change of working conditions to the compressor load.

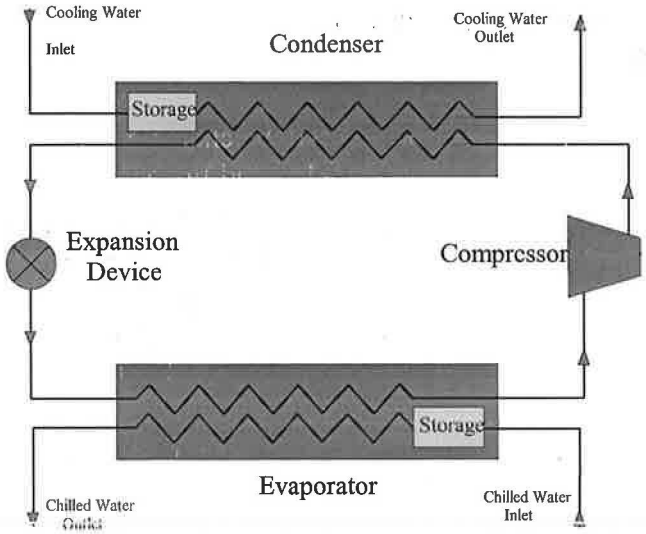

Figure-2 Schematic of chiller dynamic model

$$C_{ev}\frac{dT'_{ev,in}}{dt} = c_{wp}M_{w,ev}(T_{ev,in} - T'_{ev,in}) \quad \text{(Eq-9)}$$

$$C_{cd}\frac{dT'_{cd,in}}{dt} = c_{wp}M_{w,cd}(T_{cd,in} - T'_{cd,in}) \quad \text{(Eq-10)}$$

where, $T_{ev,in}$ and $T_{cd,in}$ are the inlet temperatures of chilled water at evaporator and cooling water at condenser, $T'_{ev,in}$ and $T'_{cd,in}$ are the inlet temperatures of chilled water and condenser cooling water after introducing dynamic effects of evaporator and condenser.

Variable-Speed Pump and Seawater Network

The variable-speed seawater pump set is simulated by a steady-state pump, a steady-state frequency inverter and a dynamic actuator of the inverter. The frequency at the outlet of the inverter is linear to the input signal from actuator. The efficiency of the inverter is included within the model of pump energy performance. The energy performance and pump characteristics at various speed are simulated using fourth-order polynomial functions as shown in equation (9) and (10). The coefficients of the equations are determined by regression using the performance data from experiments or manufacturer.

$$W_{pu}(f, M_{pu}) = \sum_{i=0}^{m}\sum_{j=0}^{n} C_{ij} f^i M_{pu}{}^j \quad \text{(Eq-9)}$$

$$P_{pu}(f, M_{pu}) = \sum_{i=0}^{m}\sum_{j=0}^{n} E_{ij} f^i M_{pu}{}^j \quad \text{(Eq-10)}$$

To avoid the difficulty of convergence which is faced in most cases when solving the equations in separate models using component-based simulation programs, the pressure-flow characteristics of the entire seawater network is simulated in one model (Figure-3). The pressure-flow balance of the seawater network is obtained by solving the pressure-flow equations of the entire network within one single model by internal iteration. The thermodynamic performance of heat exchangers is simulated by another separate model

which uses the water flow rates through heat exchangers available from the outputs of the seawater network model.

The model of the seawater network pressure-flow characteristics consists of the pressure balance equation (11), flow balance equation (12) and the equations presenting the pressure-flow characteristics of exchangers, pipe and variable-speed seawater pumps. The pressure-flow characteristics of the pipes and heat exchangers are modeled by polynomial equations and the coefficients of the equations are determined using the pressure-flow performance data measured in site. Those coefficients might be determined by the pipe and valve pressure loss equations when the details of the geographic data of the network are available.

$$P_{pu}(f, M_{pu}) - P_{pi}(M_{tot}) - P_{ex,i}(M_{ex,i}) = 0 \qquad \text{(Eq-11)}$$

$$M_{tot} = \sum_{i=1}^{2} M_{pu,i} = \sum_{i=1}^{5} M_{ex,i} \qquad \text{(Eq-12)}$$

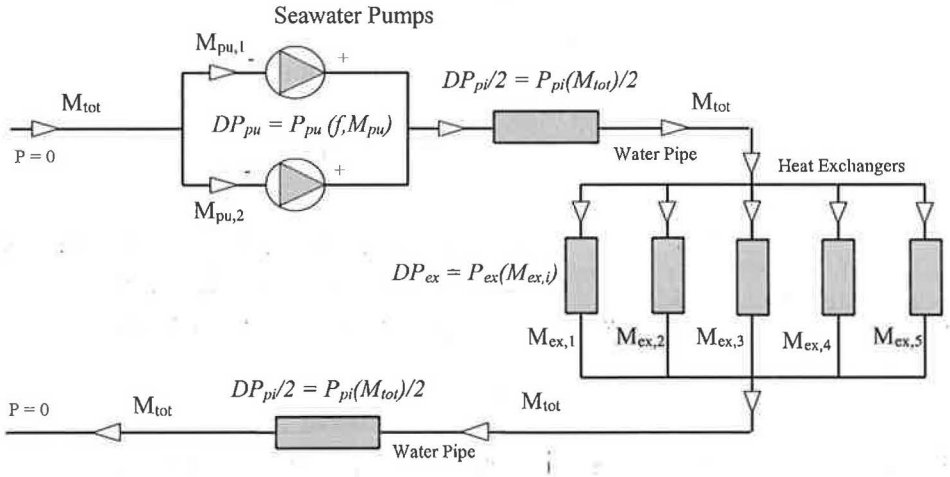

Figure-3 Schematic of seawater network model

Secondary Chilled-Water Network

The pressure-flow balance of the secondary chilled-water network is shown in Figure-4. The building is divided into five zones. The pressure-flow characteristics of the selected AHU from each zone is simulated and all the other AHUs in the same zone are considered by multiplying the flow rate of the simulated AHU with a ratio. The entire secondary chilled water network flow-pressure balance is simulated and solved by one single model similarly to avoid difficulties in convergence.

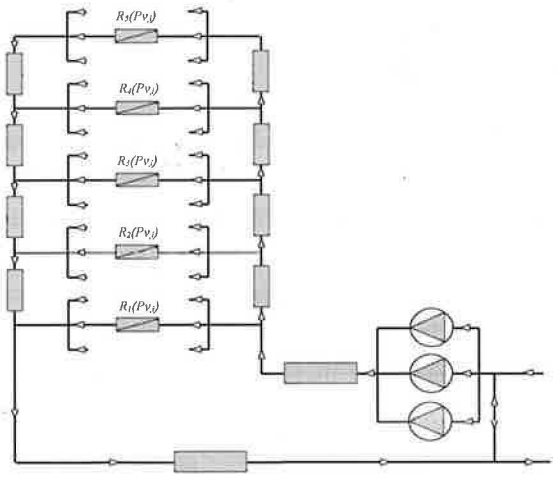

Figure-4 Schematic of secondary chilled water network model

As inputs of the network model, the positions of the two-way moderating valves are given by the actuator model controlled by the AHU supply air temperature controller, and the flow rate through the coil is computed by this network model and returned to AHU coil thermal model for AHU temperature loop simulation. The model calculates the flow resistance of the coils according to positions of associated valves.

The pressure-flow and energy characteristics of the constant speed secondary chilled water pumps are simulated by giving the pump curve and power curve. The flow resistances of the main supply and return pipes and pipes between the zones are considered to be constant.

Knowing the number of pumps in operation, the position of AHU moderating valves and the total chilled water flow rate from chillers, the network model determines the network balance and computes the water flow rates through individual AHU, the pressure at various point in the network, the flow through individual pump, the pump power consumption and the water flow rate through the bypass.

Primary Seawater Heat Exchanger

The dynamic performance of the heat exchangers is represented by one classical steady-state heat transfer model and one simple dynamic model. The heat transfer model computes the Number of Transfer Units (NTU) and heat transfer efficiency of exchanger using (13) for a counter-flow heat exchanger and then computes the steady-state outlet temperatures of two water streams.

$$\varepsilon = \frac{1-e^{-NTU\cdot(1-\frac{C_{\min}}{C_{\max}})}}{1-\frac{C_{\min}}{C_{\max}}\cdot e^{-NTU\cdot(1-\frac{C_{\min}}{C_{\max}})}} \qquad \text{(Eq-13)}$$

Two thermal storages are assumed at the seawater outlet and cooling water outlet respectively to simulate the dynamic response of an exchanger (Figure-5). Two differential equations represent the dynamic performances as shown by the equations (14) and (15).

$$C_{sea}\frac{dT_{sea,o}}{dt} = c_{w,p}M_{w,sea}(T'_{sea,o} - T_{sea,o}) \quad \text{(Eq-14)}$$

$$C_{w,cd}\frac{dT_{w,cd,o}}{dt} = c_{w,p}M_{w,cd}(T'_{w,cd,o} - T_{w,cd,o}) \quad \text{(Eq-15)}$$

where, $T_{sea,o}$ and $T_{w,cd,o}$ are the outlet temperatures of seawater and cooling water after introducing dynamic effects of an exchanger, $T'_{sea,o}$ and $T'_{w,cd,o}$ are the steady-state outlet temperatures of seawater and condenser cooling water.

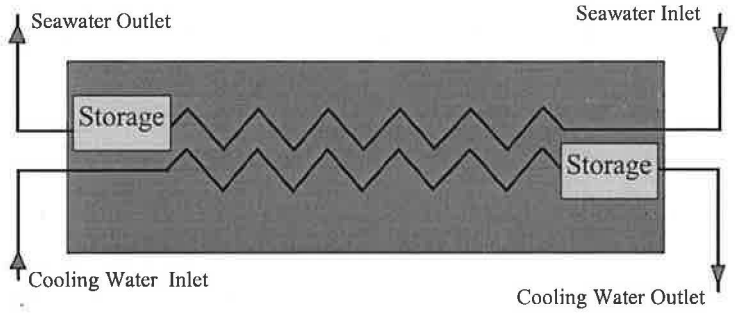

Figure-5 Schematic of heat exchanger dynamic model

Cooling Coil

A modified version of TRNSYS (A Transient System Simulation Program) [5] heating/cooling coil model developed in the IEA project Annex 17 is used. The model includes a steady-state approach and a dynamic approach [6]. A first order dynamic model is used which represents the dynamics of a coil with lumped thermal mass. A mean temperature of the coil is used which is assumed equal to the surface temperature of the coil.

The dynamic equation is based on the energy balance of the coil. Therefore the model ensures that the energy is conserved.

$$C_c\frac{dt_c}{d\tau} = \frac{t_{a,su} - t_c}{R_1} - \frac{t_c - t_{w,su}}{R_2} \quad \text{(Eq-16)}$$

where, t_c is the mean temperature of coil, $t_{a,su}$ and $t_{w,su}$ are the inlet air and water temperatures. C_c is the overall thermal capacity of the coil, R_1 and R_2 are the overall heat transfer resistances at the air and water sides.

The air and water temperatures at the outlet therefore can be computed by the heat balances of both sides:

$$t_{a,ex} = t_{a,su} - \frac{SHR(t_{a,su} - t_c)}{R_1 C_a} \quad \text{(Eq-17)}$$

$$t_{w,ex} = t_{w,su} - \frac{t_c - t_{w,su}}{R_2 C_w} \quad \text{(Eq-18)}$$

where, C_a and C_w are the capacity flow rates of air and water, SHR is the sensible heat ratio. SHR uses the same value calculated in the same inlet condition in the steady-state case using the by-pass factor method.

The model employs a detailed approach to compute the heat transfer of the coil. On the air side, two different methods are used to compute the heat transfer in dry and wet regions respectively.

Actuator, Sensor and Pipe

The actuator model is used to represent the characteristics of actuators [7]. The actuator is assumed to accelerate very quickly and then turn at constant speed. A minimum change (e.g. the sensitivity of the actuator defined as a parameter of the model) in demanded position is required to restart the actuator. The model includes the hysteresis in the linkage between actuators and valves or dampers. If a valve stem is driven by a rotary actuator, the speed of the valve stem varies with the position of the crank.

The actuator model also counts the number of 'start/stop or reversals' of an actuator and the value of 'travelled distance' of the valve (counted as 1 unit when a valve moves from its minimum position to maximum position). These figures provide indications of wear potential of an actuator/valve and hence the cost of failure or maintenance.

The dynamics of temperature and pressure sensors is simulated by using the time constant method. One first order differential equation (19) represents the dynamic characteristics of a sensor.

$$\frac{dy'}{dt} = \frac{y - y'}{T_c} \qquad \text{(Eq-19)}$$

where, y is the true value of the measured variable, y' is the measured value of the variable and T_c is the time constant.

The thermal dynamic characteristics of water pipes is simulated by using the pipe model TYPE31 using variable size segments of fluid available in the original TRNSYS package. Entering fluid shifts the position of existing segments. The mass of the new segment is equal to the flow rate the simulation time step. The new segment's temperature is that of the incoming fluid. The outlet of this pipe is a collection of the elements that are pushed out by the inlet flow.

Direct Digital Control

Unlike so-called 'perfect' models of a controller normally used to test the energy performance of control strategies, the realistic models developed represent the following functions of the BEMS:

- DDC (Direct Digital Control) functions;
- Realistic operation procedure of digital controllers.
- Supervisory control strategies;

The time scheduling of a sampling cycle is considered to be four steps: process variable sampling, control outputs computation, control signal output, and waiting time for the next sampling cycle.

The PID control function used in DDC loops uses the ideal non-interacting PID algorithm, which has the discrete form as shown by (20). The handling of the proportional term, integral term and derivative term follows the algorithm implemented in commercial Building Energy Management Systems.

$$U_k = K_p e_k + [I_{k-1} + \frac{K_p \Delta T}{2T_i}(e_{k-1} + e_k)] + K_p T_d \frac{e_k - e_{k-1}}{\Delta T} \qquad \text{(Eq-20)}$$

$$(\textit{where, } I_{k-1} + \frac{K_p \Delta T}{2T_i}(e_{k-1} + e_k) = I_k \ )$$

where, e_k, e_{k-1} are the error signals at current sampling and previous sampling, k_p is the proportional gain, T_i is the integral time, T_d is the derivative time, ΔT is the sampling interval, I_k and I_{k-1} are the integral time at the current and previous time steps, U_k is the output of PID.

System Dynamic Simulation

TRNSYS is used as the platform for the dynamic simulation of HVAC system. Figure-6 shows the schematics of the inter-connection of the component models (information diagram) in simulation.

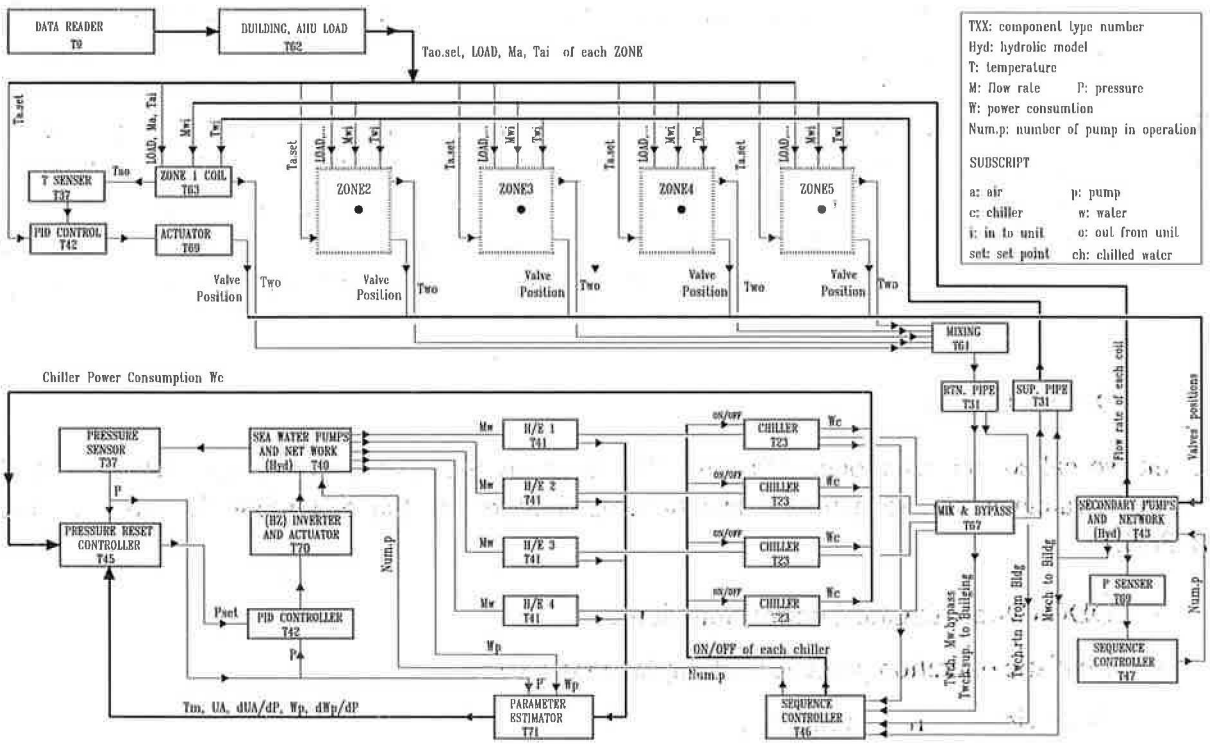

Figure-6 Schematic of TRNSYS simulation DECK

Five AHUs are simulated each of which represents the dynamic load of AHUs in one of the five zones of the entire building. The AHU outlet temperature is controlled by a digital PID controller at given set-point which is different from season to season. A two way moderating valve is used to control the water flow rate through a coil, which is driven by an actuator according to the control signal given from the temperature controller. The flow rate through each simulated AHU coil is multiplied by a factor to represent the total load of all the AHUs in the zone.

The air flow rate and AHU inlet temperatures for different seasons are given by data files during simulation as test condition, which has slightly different patterns for the AHUs in different zones to ensure the that control actions of AHUs in different zones are not simultaneous. Figure-7 shows the flow rate and AHU inlet temperature for one zone (24 hours operation) in summer season. The overall cooling load of the AHU in the entire building in four different seasons used in the simulation exercises is shown in Figure-8, which is selected referring to the actual building load in different seasons from field monitoring.

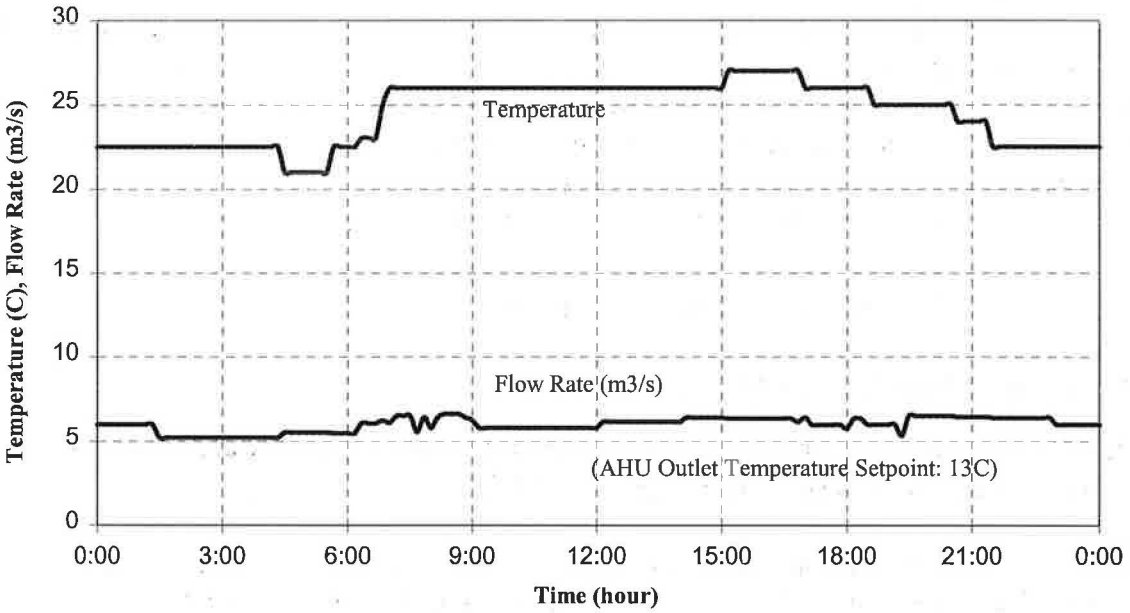

Figure-7 AHU inlet temperature and air flow rate (Summer season)

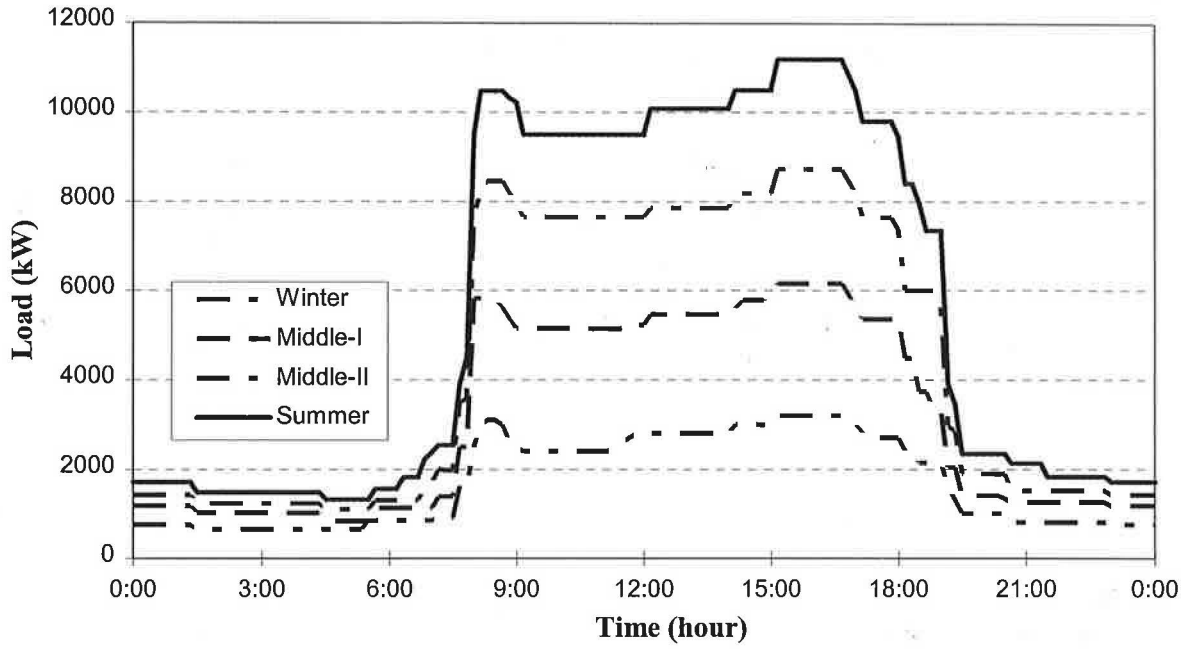

Figure-8 Total cooling load of AHUs in the building

To avoid the difficulty in convergence when solving the pressure-flow balances of chilled water network and seawater network, the pressure-flow balances of chilled water network and seawater network are simulated by separate models. The water flow rates through cooling coils and heat exchangers as the outputs of the water network models are given to the thermodynamic performance models as inputs. The temperature controller will adjust the valve positions and then the flow rate to control the temperatures at the set-points.

Central Chilling System Control Strategies

Sequence and local loop controls

Three local loop control strategies and one supervisory control strategy are used to control the system, which are simulated in the evaluation exercise.

The chiller sequence controller controls the number of chillers in operation according to a few criteria in increasing the number of chillers and reducing the number of chillers. If a negative by-pass flow over certain value for significant time, one more chiller will be switched on. If the measured total chilling load of the building is, for significant time, less than the total cooling capacity of the running chillers when one of the currently running chillers is switched off, one chiller will be switched off. Minimum time intervals for switching on one more chiller after some chiller was switched off and switching off one chiller after some chiller was switched on are set in the strategy to avoid too frequent start/stop of the chilllers. The number of seawater pumps in operation depends on the number of chillers in use, e.g. one pump is used if one or two chillers is in operation, two pumps are used if three or four chillers are used.

The sequence controller of the secondary pumps determines the number of the pump in use according to the measured pressure head at the secondary pump supply. Switch set-points for

increasing the number of pumps (from one to two and from two to three) and reducing the number of pumps (from three to two and from two to one) are set as the parameters of the controller. Minimum interval in changing the number of pumps in operation is introduced to avoid that the pumps are stitched on and off frequently.

One PID pressure controller is used to maintain the seawater pressure head at the inlet of the heat exchangers at its set-point, which is reset by the seawater pressure supervisory control strategy. The pressure controller senses the pressure at the inlet of heat exchangers and adjust the frequency output of the frequency inverters using the PID algorithm.

Optimal Pressure Set-point Reset

The on-line near optimal reset of the seawater pressure set-point is achieved by a derivative control strategy and an adaptive strategy control strategies [8]. The derivative control strategy resets the pressure set-point by adjusting the pressure set-point according to the estimated derivative of the total power with respect to seawater pressure. The adaptive strategy is used to identify the system parameters essential for the control strategies.

The derivative control adapts the knowledge of operators in supervising and optimizing a controlled variable. The controller estimates the derivative of total power (W_{tot}) with respect to the seawater pressure (P) across the heat exchanger. If the value of the derivative is positive, the pressure should be reduced. In contrast, the pressure should be increased if the derivative has a negative value. The pressure will approach the optimal point when the derivative approaches zero at a certain building load or cooling load. In the actual operation of a building chilling system, the adjustment will be a regular task for a controller to maintain a zero derivative value, since the load is changing.

The derivative of the total power can be obtained from the derivatives of pump power (W_p) and chiller power (W_c) with respect to pressure, as represented by equation (21).

$$\frac{\partial W_{tot}}{\partial P} = \frac{\partial W_p}{\partial P} + \frac{\partial W_c}{\partial P} \qquad \text{(Eq-21)}$$

In order to estimate the derivative of total power using the system information available from conventional BEMS monitoring systems, a few assumptions and simplifications are introduced. The controller finally estimates the derivative of the pump power using the formula shown by (22). To properly adjust the pressure, the controller should identify the derivatives of pump power and the heat transfer coefficient with respect to the pressure, and should obtain the chiller energy power, mean temperature difference and heat transfer coefficient.

$$\frac{\partial W_{tot}}{\partial P} \approx \frac{dW_p}{dP} + C_c \cdot W_c \cdot \left(-\frac{T_m}{UA}\right) \cdot \frac{dUA}{dP} \qquad \text{(Eq-22)}$$

Having the derivative of the total power with respect to the pressure, the controller adjusts the pressure set-point with a change rate determined by the derivative function shown in equation (23). Where, dP_{set}/dt is the change rate for pressure set-point adjustment and K is a positive constant (proportional gain).

$$\frac{dP_{set}}{dt} = -K \cdot \left(\frac{\partial W_{tot}}{\partial P} \right) \qquad \text{(Eq-23)}$$

Besides the chiller power, heat transfer coefficient and mean temperature difference, two derivatives (derivatives of heat transfer coefficient and pump power with respect to pressure) are essential in order to identify the derivative of total power. It is difficult to obtain reliable values of these derivatives directly by taking the ratio of measured increment of heat transfer coefficient, pump power and pressure, particularly for the derivative of heat transfer coefficient, due to the effects of dynamics.

Recursive Least-Squares (RLS) estimation with exponential forgetting is implemented to identify the derivatives of the heat transfer coefficient and pump power with respect to the pressure. It is also used as a filter in identifying the heat transfer coefficient. Second order models for the pump power and heat transfer coefficient are used, which are shown by equation (24) and (25).

$$UA(t) = \left[b_0(t),\ b_1(t),\ b_2(t)\right] \cdot \left[1,\ P(t),\ P(t)^2\right]^T \qquad \text{(Eq-24)}$$

$$W_p(t) = \left[c_0(t),\ c_1(t),\ c_2(t)\right] \cdot \left[1,\ P(t),\ P(t)^2\right]^T \qquad \text{(Eq-25)}$$

where, $b_0(t), b_1(t), b_2(t), c_0(t)$ $c_1(t), c_2(t)$ are time dependent parameters to be identified.

Four estimators for heat transfer coefficient are used, one for each chiller exchanger. One estimator requests the water temperatures at the inlet and outlet of exchanger, and the pressure. The estimator for pump power shifts among four different sets of coefficients and matrix, each of which corresponding to one combination of chiller and pump. When a new combination starts, the estimator uses the last values of this combination as the initial values of the coefficients and matrix. At each sampling step, the derivatives of heat transfer coefficient and pump power, and the heat transfer coefficient are estimated using the coefficients identified.

Performance Test and Evaluation of Control Strategies

The simulation exercise was performed to test the dynamic response and energy performance of the control strategies under various loads. Four one-day tests were performed in each of the four cases. In the first test, the pressure is reset by the optimal reset strategy. In the following two tests, the pump was set to be minimum or maximum speed. The fourth test was an 'ideal reset' test, while the pressure was reset by the derivative control using the 'true' performance data of exchangers and pumps to validate the optimal reset strategy.

Figure-9 shows the pressures and seawater pump frequency of optimal reset strategy test for the 'Summer Case'. In night operation mode, the pump was set to the minimum speed, whilst only one chiller was in operation (Figure-10). The pressure and frequency had a peak at the beginning of the day operation mode, which was the result of high start chiller load and the response of the strategy to the sudden load change. It disappeared quickly, which shows that the stability of the strategy is acceptable. During the main part of the day, the reset controller

regulated the pressure according to the change of the building cooling load, while four chillers were in operation. It can be observed that the pressure changed following the change of chiller load. A peak appeared around 16:00pm as the chiller load. Near the end of the day, the controller set the pressure at a low level, since two chillers worked at partial load.

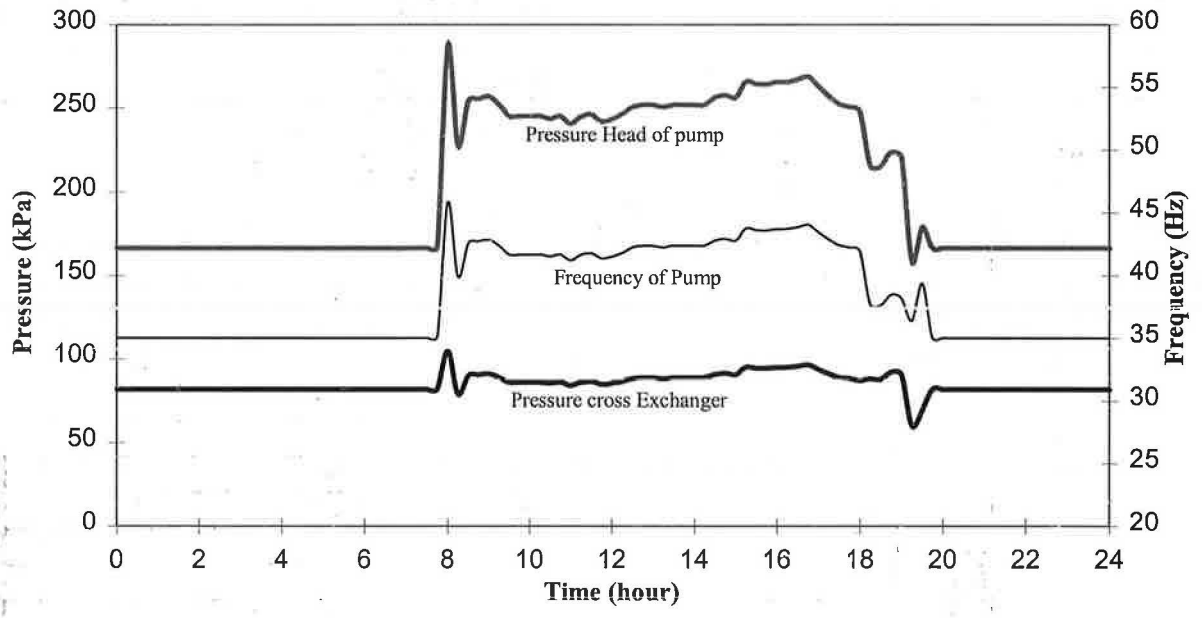

Figure-9 Seawater pressures and pump frequency (Summer case)

The energy statistics (Table-1) shows that the optimal pressure set-point reset strategy saved 3.83% of the total electricity consumption in comparison with the consumption when setting the pump at minimum speed, and saved 3.68% of the total electricity consumption in comparison with the electricity consumption when setting the pump at maximum speed. The electricity consumed when using optimal reset strategy was only 0.03% higher than that using the 'ideal control'.

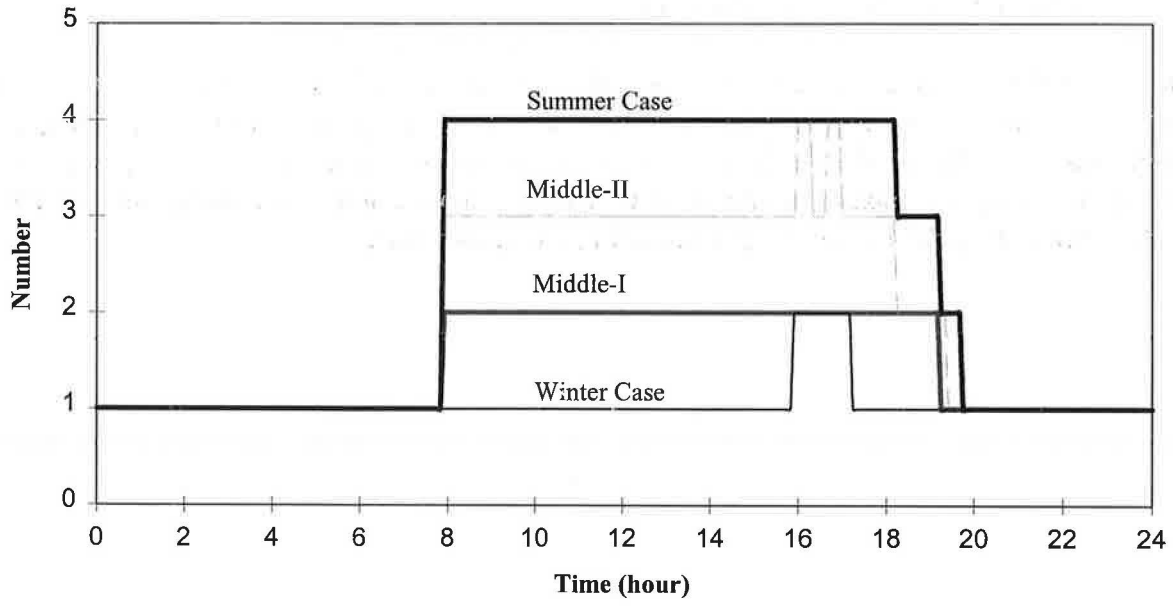

Figure-10 Number of chillers in operation in four tests

Table-1 Electricity Consumption at Various Loads

Test Case	Control Strategy	Seawater Pump (kWh)	Chiller (kWh)	Chiller + Seawater Pump (kWh)	Comparison with Adaptive Reset (%)
Winter *(one day)*	Minimum	1752.8	11638.9	13391.7	0.00
	Maximum	4552.8	10755.6	15308.3	+14.31
	Adaptive Reset	1788.9	11602.8	13391.7	-
	Ideal Reset	1788.9	11591.7	13380.6	-0.01
Middle-I *(one day)*	Minimum	1750.0	22419.4	24169.4	+5.15
	Maximum	4500.0	19886.1	24386.1	+6.10
	Adaptive Reset	2388.9	20594.4	22986.1	-
	Ideal Reset	2388.9	20577.8	22966.7	-0.08
Middle-II *(one day)*	Minimum	2500.0	30483.3	32983.3	+1.70
	Maximum	6505.6	27877.8	34383.3	6.02
	Adaptive Reset	3100.0	29330.6	32430.6	-
	Ideal Reset	3111.1	29305.6	32416.7	-0.04
Summer *(one day)*	Minimum	2580.6	40555.6	43136.1	+3.83
	Maximum	6716.7	36355.6	43072.2	+3.68
	Adaptive Reset	3705.6	37877.8	41583.3	-
	Ideal Reset	3725.0	37844.4	41569.4	-0.03

Figure-11 shows the pressures and seawater pump frequency of optimal reset strategy for 'Middle-II' case. In night operation mode, the pump was at minimum speed. During the main part of the day, the reset controller regulated the pressure according to the change of the building cooling load, while three chillers were in operation. Around 16:00pm, there was an obvious increase of pump frequency due to the peak of chilling load. The two shocks occurred were the response of the control to the changes of chiller number between three and four. Before the end of the day, two chillers worked at high load, the controller set a high frequency for the single pump in operation.

The optimal reset pressure set-point reset strategy saved 1.7% of the total electricity in comparison with the electricity consumption when setting the pump at minimum speed, and saved 6.02% of the total electricity in comparison with the electricity consumption when setting the pump at maximum speed. The electricity consumed when using optimal reset strategy was 0.04% higher than that when using the 'ideal control'.

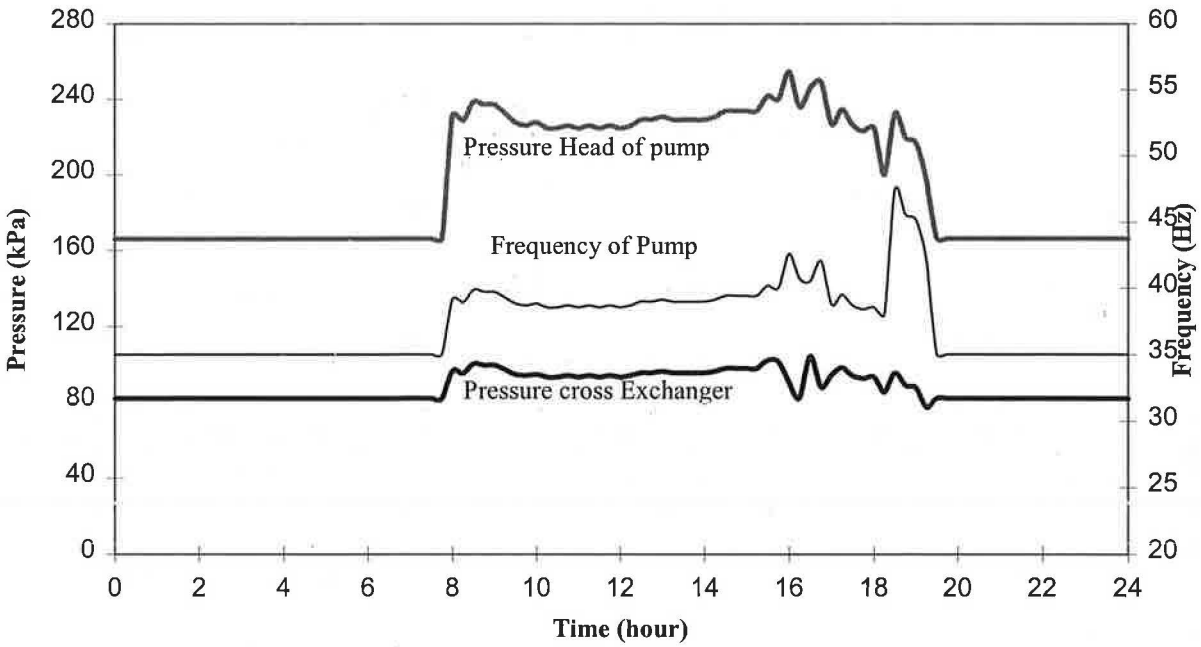

Figure-11 Seawater pressures and pump frequency (Middle-II)

Figure-12 shows the pressures and seawater pump frequency of optimal reset strategy for 'Middle-I' case. In night operation mode, the pump was at minimum speed. During the day, two chillers were used. There was a sudden reduction of pressure when the second chiller started and the pressure regulator had some delay in response to this change (increase pump speed). The reset controller regulated the pressure according to the change of the building cooling load during the day, while there were some obvious changes of pressure setting around 13:00pm, caused by the sequencing control of secondary pumps resulting significant changes of chiller load. The controller reduced the pressure setting near the end of the day since two chillers operated at low load.

The optimal pressure set-point reset strategy saved 5.15% of the total electricity in comparison with the electricity consumption when setting the pump at minimum speed, and saved 6.1% of the total electricity in comparison with the electricity consumption when setting the pump at maximum speed. The electricity consumed when using optimal reset strategy was 0.08% higher than that when using the 'ideal control'.

Figure-13 shows the pressures and seawater pump frequency of optimal reset strategy for 'Winter Case'. Nearly all day, the pressure was set to be at minimum due to the low chiller load. There was a pressure rise for a short period at the beginning of office hours due to the large cooling load of the AHU at starting. The pressure was set to be higher around 15:00pm due to increase of building load. Between 16:00pm and 17:00pm, two chillers were in operation. the frequency of the pump was at peak. The pressure was reduced since the load was shared by two chillers resulting in low load for each chiller.

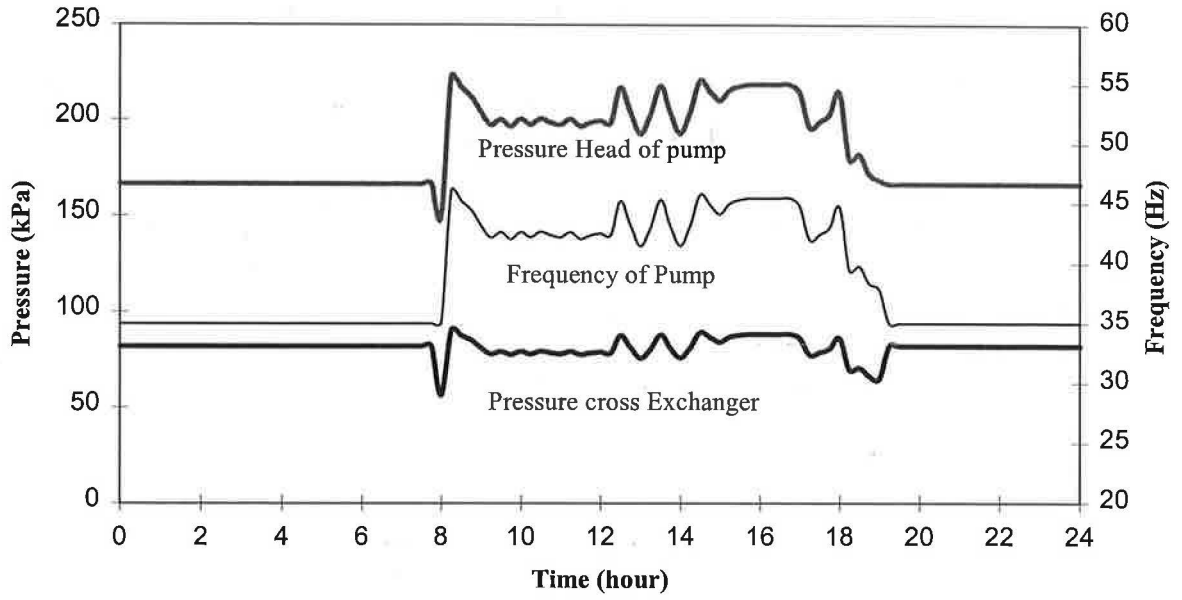

Figure-12 Seawater pressures and pump frequency (Middle-I)

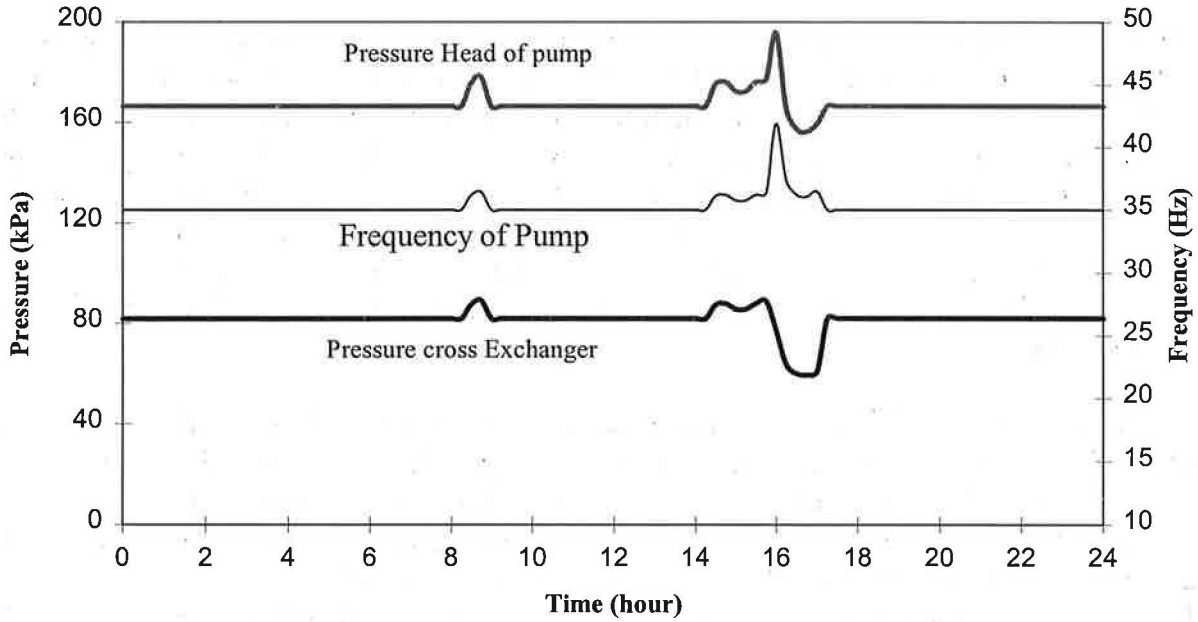

Figure-13 Seawater pressures and pump frequency (Winter season)

The optimal pressure set-point reset strategy had no saving on the total electricity in comparison with the electricity consumption when setting the pump at minimum speed since the optimal control was very close to the minimum setting. But it saved 14.31% of the total electricity in comparison with the electricity consumption when setting the pump at maximum speed. The electricity consumed when using optimal reset strategy is 0.01% higher than that when using the 'ideal control'.

Summary and Conclusions

Simulation exercises show that the dynamic system simulation is a convenient and suitable tool in testing and evaluating the control performance of large central chilling systems and their on-line control strategies. However, simulation tests show that there are difficulties in convergence when component models representing both the thermodynamic and hydraulic performances of individual component are integrated to simulate the realistic (e.g. thermodynamic, hydraulic, etc.) performances using the component-based simulation programs such as TRNSYS. The use of separate models to handle the pressure-flow balance of entire water networks is one solution for such problem.

The test results also show that significant energy saving in seawater-cooled central chilling systems can be achieved by properly resetting the pressure set-point and the seawater pump speed using on-line optimal control strategies. These on-line control strategies can be tested, commissioned and pre-tuned by using them to control the living chilling systems in simulation.

Acknowledgment

This paper presents the contribution of the authors to the IEA (BCS) joint research project Annex 30 (Bringing Simulation into Application). The research work in The Hong Kong Polytechnic University is financially supported by the university research grant.

References

1. Wang S.W., Lebrun J. and Nusgens P. "Use of Real Time Simulation for Testing Building Energy Management Systems.", CLIMA 2000, London, UK, November , paper no. 309, 1993.
2. Wang S.W and Burnett J. 'BEMS Control Strategies: Evaluation of realistic Performance by Computer Simulation', <Building Services Engineering Research and Technology>, Volume 17, No.1, 1996
3. S.W. Wang, J.B. Wang and J. Burnett 'A Mechanistic Model of Multi-Stage Centrifugal Chillers for System Simulation', Paper submitted to <International Journal of Refrigeration>, 1996
4. V.P. Carey, *Liquid-Vapor Phase-Change Phenomena*, pp. 368-372, Hemisphere, New York, 1992.
5. S.A. Klein, W.A. Beckman, J.W. Mitchell , etc. "TRNSYS - A Transient System Simulation Program (Reference Manual)", University of Wisconsin-Madison, USA, July, 1994
6. Lebrun J., Ding X., Eppe J.P. and Wasacz 'Cooling Coil Models to be Used in Transient and/or Wet Regimes - Theoretical Analysis and Experimental validation', IEA (BCS) Annex 17 Report, Liege, Belgium (1990)

7. Haves P. and Dexter A.L. 'Simulation of Local Loop Controls', Proc. Building'89, IBPSA, Vancouver (1989)
8. Wang S.W and Burnett J. 'Adaptive and Derivative Control for Optimizing Variable-Speed Pumps of Seawater-Cooled Chilling Systems', Paper submitted to <HVAC&R Research Journal>, 1996